



Neurochemical imaging of selenium homeostasis in the brain under nutritional deficiency

Journal:	<i>Journal of Neurochemistry</i>
Manuscript ID:	JNC-E-2008-0185
Manuscript Type:	Original Article
Date Submitted by the Author:	14-Feb-2008
Complete List of Authors:	Savaskan, Nicolai; Brain Research Institute, Dept. of Neuromorphology Eyüpoglu, Ilker; University of erlangen, neurosurgery hahnen, eric; university of cologne, human genetics kühn, hartmut; charite university medical school berlin, biochemistry
Keywords:	autoradiography, nutritional gene expression, radiotracer, selenoproteins, microarray chip analysis, GPx

Neurochemical imaging of selenium homeostasis in the brain under nutritional deficiency

Ilker Y. Eyüpoglu¹, Eric Hahnen², Hartmut Kühn³ and Nicolai E. Savaskan^{4*}

¹Department of Neurosurgery, University of Erlangen-Nuremberg, D-91054 Erlangen, Germany. ²Institute of Human Genetics, Institute of Genetics and Center for Molecular Medicine Cologne (CMMC), University of Cologne, Germany. ³Institute of Biochemistry, Charité University Medical School Berlin, Germany. ⁴Brain Research Institute, Department of Neuromorphology, Swiss Federal Institute of Technology (ETH) and University Zürich, Winterthurerstrasse 190, Zürich, Switzerland.

Short Title: Neurochemical imaging of selenium in the brain

Number of words: (including abstract and references)

Number of figures: 5

Number of pages: 19 (excluding figures)

***Corresponding Author:**

Dr. Nicolai E. Savaskan
Brain Research Institute
Department of Neuromorphology
Swiss Federal Institute of Technology (ETH) & University of Zürich
Winterthurerstrasse 190
CH-8057 Zürich
Switzerland
Phone: +41 765 211 322
Fax: +41 44 635 33 03
E-mail: savaskan@gmx.net

1
2
3 Neurochemical imaging of selenium in the brain
4
5

6 **Abstract**
7

8 Dietary selenium (Se) and selenoproteins play a pivotal role in the brain.
9 Selenium deficiency with subsequent selenoprotein depletion or targeted gene
10 disruption causes severe neurological deficits. Although not the highest Se content, the
11 brain, in addition to testis, is a privileged organ with high priority for selenium uptake
12 under low nutritional selenium supply. To address the critical privilege of selenium in the
13 brain and characterize nutritional effects on the selenoproteome, we applied the
14 radiotracer ^{75}Se *in vivo* and imaged Se incorporation by autoradiography. Selenium was
15 region-specifically incorporated and in addition to choroid plexus neuron-rich areas such
16 as hippocampus, cortex and cerebellar nuclei showed highest Se levels. These data
17 were corroborated by microarray analysis and selenoprotein expression profiles in
18 human and rodent brains. In contrast, testis showed almost uniform parenchymal Se
19 incorporation. Low Se status led to increased selenium uptake in all regions of the grey
20 matter as well as Se enrichment in choroid plexus. Taken together, our study revealed a
21 unique Se uptake pattern in the brain with hippocampus, cortex, cerebellum and choroid
22 plexus as Se privileged regions. These data suggest the requirement of certain
23 selenoproteins for proper neuronal function.
24
25
26
27
28
29
30
31
32
33
34
35
36
37
38
39
40
41
42
43
44
45
46
47
48
49
50
51
52
53
54
55
56
57
58
59
60

Key words: autoradiography, nutritional gene expression, radiotracer, GPx4/PHGPx,
Microarray chip analysis, selenoproteins.

Abbreviations: ApoER2, apolipoprotein E receptor 2; CSF, cerebrospinal fluid; Cx,
cortex; GPx, EC, entorhinal cortex; DG, dentate gyrus; glutathione peroxidase; RDA,
recommended daily allowance; Se, selenium; SePP, selenoprotein P.

Neurochemical imaging of selenium in the brain

Introduction

The homeostasis of essential inorganic elements in the central nervous system shows distinct differences in comparison with other organs (Spector 1989, Takeda et al., 1994). In particular, the trace element selenium (Se) is an essential micronutrient required for normal brain function (for review see Chen and Berry, 2003; Schweizer et al., 2004). The micronutrient Se is ingested in form of four different chemically species (selenomethionine, selenocysteine, selenate and selenite) (Andersen & Nielsen 1994). However, in disparity to most other trace elements, selenium occurs in proteins in the form of selenocysteine (Sec), the 21st amino acid (Berry et al., 1991; Hatfield and Gladyshev, 2002). Its specific insertion into selenoproteins is conserved in all three taxa of bacteria, archaea and eukaryotes and requires in-frame UGA codons, which normally specify termination of translation (Berry et al. 1991, Caban & Copeland 2006). Employing this feature and its distinct Selenocysteine Insertion Sequence (SECIS) as tools for bioinformatical screening of the genomes, 25 selenoproteins could be identified in animal kingdom and in humans (Kryukov et al. 2003; Castellano et al. 2001; Lescure et al. 1999).

Recent findings showed that the selenium (Se) status is critical for proper brain function and mitigated brain Se levels cause neurological deficits and disorders during development and in adults (Ramaekers et al., 1994; Arthur et al., 1997; Benton, 2002; Savaskan et al., 2003). However, at the expense of other organs, brain and testis are two privileged organs which maintain high Se levels even under selenium deficiency. Although not the highest selenium concentration is found in the brain when compared to other organs, brain tissues show a high priority for selenium uptake and retention in the case of dietary selenium deficiency. The preferential supply of the brain with this trace element in prolonged periods of selenium deficiency suggests specific Se uptake and storage mechanism in this organ (Schomburg et al., 2003; Hill et al., 2003). Selenoprotein P (SEPP) has been suggested to play a major role for Se transport, supply and organ storage (Burk and Hill, 2005; Renko et al., 2007). Expression of selenoproteins in the brain depends on the supply with the trace element and thus, higher susceptibility to glutamate toxicity and neuropathological alterations following Se deficiency may be related to altered selenoprotein expression (Savaskan et al., 2003).

1
2
3 Neurochemical imaging of selenium in the brain
4
5

6 Knowledge on the selenoproteome distribution in the brain has been limited for a
7 long time and systematic expression data for selenoproteins were restricted to GPx1,
8 SePP (Saijoh et al., 1995) and GPx4 (Borchert et al., 2006; Savaskan et al., 2007). A
9 recent comparative selenoproteome expression study indicated that the complete
10 selenoproteome is expressed in the adult mouse brain but functional relevance of these
11 expression data remain elusive (Zhang et al., 2007).
12
13
14
15

16 The present work was based on a classic tool in selenium research, utilizing the
17 radiotracer ^{75}Se combined with high resolution autoradiographic imaging and a
18 microarray and RT-PCR based selenoprotein expression profiling approach. Former
19 investigations with the application of ^{75}Se (Pullen *et al.* 1995, Pullen *et al.* 1996, Trapp &
20 Millam 1975) and studies on selenium uptake and homeostasis in the brain were based
21 on manual separation of gross anatomical parts (Behne et al., 1982, 1988) which
22 hindered spatial resolution at the regional and cellular level. In this work, we used
23 autoradiographic imaging for the quantification and determination of ^{75}Se -distribution in
24 the brain at the regional level, gaining new information about the regional priorities in
25 the hierarchy of cerebral selenium homeostasis. We found that selenium is incorporated
26 in specific brain regions, whereas testis, another Se privileged organ, shows a uniform
27 parenchymal Se distribution. In addition microarray profiles, RT-PCR analysis and
28 immunohistochemistry confirmed the presence of essential selenoproteins in neuron
29 rich regions of the brain.
30
31
32
33
34
35
36
37
38
39
40
41
42
43
44
45
46
47
48
49
50
51
52
53
54
55
56
57
58
59
60

Neurochemical imaging of selenium in the brain

Materials and Methods

Animal treatment, radiolabeling and sample preparation

The animal experiments were carried out in accordance with the German and European legislation on animal protection. A total number of 8 adult male Wistar rats (Charles River, Sulzfeld, Germany) were used and were maintained under local regulations as described (Savaskan et al., 2003). Selenium-deficient diet containing a maximum of 2–5 µg Se/kg, and selenium adequate controls received a selenium-adequate diet according to RDA in humans, which consisted of the same basal diet with 300 µg Se/kg added as sodium selenite (MP Biomedicals, formerly ICN Biochemicals, Cleveland, Ohio, USA). Analysis of selenium concentrations in the diets was performed as formerly described (Behne et al. 1994). The animals were labeled *in vivo* by intraperitoneal injection of 0.5 ml of [⁷⁵Se]-selenite solution containing 1 µg selenium. Anaesthesia was performed with Isofluran (CuraMED Pharma GmbH, Karlsruhe, Germany) and rats were sacrificed by injection of an overdose of Nembutal (Sanofi Pharma, Munich, Germany). Testis together with epididymides and brain were prepared, immediately shock frozen in liquid nitrogen and stored at -80 °C.

Neurochemical imaging and autoradiographic analysis

Brain and testis tissue were cryocut and saggital cryosections of 10 µm and 12 µm were prepared and placed on SuperFrost® Plus glass slides (Menzel, Braunschweig, Germany). After autoradiographic exposure, Nissl staining was performed with cresyl violet. The radionuclide ⁷⁵Se has a half-life of 119.8 days and decays by electron capture into stable ⁷⁵As. The spatial resolution of the imaging analyzer amounts to 50 x 50 micrometer². For the autoradiographic imaging of the ⁷⁵Se, slides were exposed to Kodak X-OMAT AR X-ray films for 7 to 30 days. Color coding and quantification of ⁷⁵Se per area was performed with Image J x1.29 (NIH, USA).

Microarray analysis and data acquisition

Transcriptome-wide analysis of total RNA isolated from rat OHSCs was performed in triplicate (n=3) using Affymetrix RAE230 rat expression arrays using standard techniques according to the manual guidelines. Transcript level estimation was performed by fluorescence density measurements on RAE230 chip arrays and expressed as arbitrary units.

Neurochemical imaging of selenium in the brain

RNA isolation and selenoproteome analysis by RT-PCR.

Total RNA from brain tissues was extracted using RNAeasy mini kit (Qiagen, Hilden, Germany). Human hippocampi were obtained from epilepsy surgery. For scientific use of tissue specimens, informed consent was obtained from each patient and approved by the local Ethics Committee of the University of Erlangen. Rat, mouse and human organotypic hippocampal slice cultures (OHSCs) were prepared and maintained according to the interface technique as described in detail (Eyüpoglu et al., 2006). RNA isolation was performed using the RNeasy Mini Kit (Qiagen, Hilden, Germany). For non-quantitative analyses, reverse transcription (RT) was performed using oligo dT primers and 1 µg of total RNA by applying the SuperScript First-Strand Synthesis System (Invitrogen, Karlsruhe, Germany). 2 µl of each 21 µl RT reaction was used for each RT-PCR. Rat, mouse and human selenoprotein cDNA were amplified using the following primer pairs: Sepp-fwd-rat (TGC CAC AAA CCA TTT CAT CC), Sepp-rev-rat (ATT ACG AGC TAT CCA ACA GA); Gpx1-fwd-rat (CAT CAG GAG AAT GGC AAG AA), Gpx1-rev-rat (ATC GGG TTC GAT GTC GAT G); Sep15-fwd-rat (CGT TTC AAG CGG TGT CTG CT), Sep15-rev-rat (CGT TTC AAG CGG TGT CTG CT); m/cGpx4-fwd-rat (GAG ATG AGC TGG GGC CGT CTG A), nGpx4-fwd-rat (AGT TCC TGG GCT TGT GTG CAT CC), Gpx4-rev-rat (ACG CAG CCG TTC TTA TCA ATG AGA A); Sepw-fwd-rat (CCT GGA CAT CTG TGG CGA), Sepw-rev-rat (AGC CTT CAG GAC CCT GCC T); Sepp-fwd-mouse (TGC CAC AGA ACA TTT CAT C), Sepp-rev-mouse (TTA CAA GCT ATC CAA CAG A); Gpx1-fwd-mouse (CAC CAG GAG AAT GGC AAG AA), Gpx1-rev-mouse (GTC AGG TTC GAT GTC GAT G); Sep15-fwd-mouse (CGT TTC AAG CGG CGT CTG CT), Sep15-rev-mouse (CGT TTC AAG CGG TGT CTG CT); m/cGpx4-fwd-mouse (CGC CTG GTC TGG CAG GCA CCA), nGpx4-fwd-mouse (AGT TCC TGG GCT TGT GTG CAT CC), Gpx4-rev-mouse (ACG CAG CCG TTC TTA TCA ATG AGA A); Sepw-fwd-mouse (CCT GGA CAT TTG TGG CGA GG), Sepw-rev-mouse (GAG CTT TCA GGA CCC TGC CT); Seps-fwd-rat (TCT GGA GCC TGA TGT TGT TG), Seps-rev-rat (TCT TCT TCC TGA GGC CTT CC); Sepr-fwd-rat (GCC AGG CGT CTA CGT GTG T), Seps-fwd-mouse (TCT GGA ACC TGA TGT TGT TG), Seps-rev-mouse (TCT TCT TCC TGA GGC CTT CC); Sepr-fwd-mouse (GCC AGG TGT CTA CGT GTG T), Sepr-rev-mouse (CTT GCC ACA GGA CAC CTT TA); Sepr-rev-rat (CTT GCC ACA

1
2
3 Neurochemical imaging of selenium in the brain
4
5

6 GGA CAC CTT TA); Sepp-fwd-human (TGT CAT AGA AAT ATT GAC TC), Sepp-rev-
7 human (CTG CTA ATT ATC CAA CAG A); Gpx1-fwd-human (CAT CAG GAG AAC
8 GCC AAG AA), Gpx1-rev-human (GTC AGG CTC GAT GTC AAT G); Sep15-fwd-
9 human (TGC TTC AAG CGG TGT CTG CT), Sep15-rev-human (CTG AAC CAC GGA
10 CAT ACT TG); Gpx4-fwd-human (TAC CGG GGC TTC GTG TGC AT), Gpx4-rev-
11 human (TGA TGG CAT TTC CCA GGA TGC); Sepw-fwd-human (CCT GGA CAT CTG
12 CGG CGA), Sepw-rev-human (AGG TCC CTG GAC TCT GCC TT); Seps-fwd-human
13 (TGT GGA ACC TGA TGT TGT TG), Seps-rev-human (TCT TCC TCC TGG GGC TTC
14 TT); Sepr-fwd-human (ACC TGG CGT TTA CGT GTG TG), Sepr-rev-human (CTT GCC
15 ACA GGA CAC CTT CA); For TR1, primers were designed which detect rat, mouse and
16 human TR1 orthologues: TR1-fwd (GAT CTT TTC TCC TTG CCT TAC), TR1-rev (GAT
17 GTA AGG CAC ATT GGT CTG). PCR conditions were as follows: 5 min initial
18 denaturation (94°C), followed by 36 cycles (94°C for 45 sec, 54°C to 60°C for 45 sec,
19 72°C for 45 sec) and final extension (72°C for 5 min). PCR products were visualized on
20 2% agarose gels by ethidium bromide staining.
21
22

23 **Immunohistochemistry.**
24

25 For immunohistochemical staining, rats were perfused with 4 % (w/v) p-formaldehyde
26 and immersion fixed overnight. Sections were prepared on a McIlwain vibratome,
27 quenched with NH₄Cl for 15 min and blocked with 10 % goat serum/ 0.1 % Saponin in
28 PBS for 1 h at room temperature. Blocked sections were exposed to the primary
29 monoclonal anti-GPx4 antibody overnight at 4°C. After washing in 0.1 % Saponin/PBS,
30 sections were incubated at +4°C with a fluorescent anti-mouse IgG (Molecular Probes,
31 Leiden, The Netherlands).
32
33
34
35
36
37
38
39
40
41
42
43
44
45
46
47
48
49
50
51
52
53
54
55
56
57
58
59
60

Neurochemical imaging of selenium in the brain

Results

Region-specific distribution of Se in the brain.

First, we studied global Se incorporation in the brain under different nutritional states. Rats were fed with special Torula yeast-based diets, containing adequate levels of sodium selenite (Se+) equivalent to the RDA in humans, or with selenium-deficient diet with maximum levels of 2-5µg/kg (Se-). Seven days after radiotracer application, both groups showed significant differences in Se incorporation in the brain (**Fig. 1**). The autoradiograms of tissue sections from animals fed with the selenium-adequate diet showed weak and ubiquitous ⁷⁵Se incorporation levels in white and grey matter regions as well as less total activity in contrast to brain sections of selenium deficient rats (**Fig. 1A, B**). Solely choroid plexus gave strong signals in Se adequate fed rats (**Fig. 1A**). In contrast, selenium deficient brains displayed a spatially restricted Se incorporation pattern with strongest signals in grey matter structures such as hippocampus (CA1-CA3 and dentate gyrus), cerebral and cerebellar cortex, whereas signals in white matter such as commissure anterior, corpus callosum or spinal cord were lower (**Fig. 1B**). Detailed quantitative analysis of ⁷⁵Se incorporated levels in the brains of Se depleted rats was subsequently performed on color coded images. Yellow-white color indicates regions with high ⁷⁵Se accumulation while black encodes for low radiotracer activity (**Fig. 2**). In general, Se distribution was lower in white matter regions than in grey matter. However, distinct areas within the grey matter showed quantitatively higher Se activity, indicating that Se is preferentially and quantitatively incorporated in neuronal cell layers rather than ubiquitously distributed. The CA1-CA3 regions, dentate gyrus, cortex and granular cell layer of the cerebellum exhibited highest ⁷⁵Se signals (**Fig. 2C**). Interestingly, comparative evaluation of 10 distinct brain regions revealed choroid plexus as the highest Se containing region (**Fig. 2C**).

The values of the ⁷⁵Se activity per area showed significant differences between testis and the three main parts of the epididymidis (**Fig. 3A**). Considering the variations of histological procedure and sectioning, highest ⁷⁵Se activity was found in the testis compared to the epididymidis. Within testis, highest Se levels were located in the seminiferous tubules, whereas the interstitium showed only moderate levels (**Fig. 3B**). Within seminiferous tubules it was possible to differentiate between the lumen and the

Neurochemical imaging of selenium in the brain

peripheral edge of the tubule, but sufficient resolution for visualizing single spermatozoae was not reached.

Candidate selenoproteins expression in the brain.

Our former autoradiogram studies indicated that with exception of choroid plexus, neuron-rich regions were heavily labeled for Se, suggesting neurons as the main cellular target for selenium incorporation. Since most of the nutritionally available Se is metabolized and incorporated in selenoproteins, we hypothesized that prominent Se incorporation in grey matter is correlated with the expression of selenoproteins (Jakubla et al., 2005; Yant et al., 2004; Borchert et al., 2006).

Initially, we evaluated the basal selenoprotein gene expression levels in the hippocampus, an anatomical region which has shown comparatively high ^{75}Se incorporation in our experimental settings and is known for the presence of enriched neurons and fewer glial cells. By employing rat organotypic hippocampal brain slices cultured under standard conditions, a transcriptome-wide microarray analysis (Affymetrix RAE230) revealed expression of 19 selenoprotein genes (**Fig. 4**), while 5 selenoprotein genes were not expressed at significant levels (Smcp, Dio1, Dio3, GPx2, Gpx6). A comparative analysis revealed 5 selenoprotein genes (SEPP, GPx1, SEP15, GPx4, SEPW) to be predominantly expressed in the rat hippocampus. Expression of these selenoprotein genes as well as the moderately expressed SEPS, TRx1 and SEPR was subsequently corroborated in mouse and human hippocampal tissue. Expression of these selenoprotein genes was subsequently corroborated in mouse and human hippocampal tissue (**Fig. 5A**). To further test selenoprotein expression on the cellular level, we performed immunocytochemistry and subsequent confocal evaluation. One candidate selenoprotein has been therefore evaluated and immunostaining revealed that GPx4 is mainly distributed in cortical neurons and their dendrites (**Fig. 5B**).

Neurochemical imaging of selenium in the brain

Discussion

To our knowledge this study represents the first spatial analysis of the trace element Se in the brain under different nutritional status. We showed that two Se privileged organs, brain and testis, incorporate Se in a region-specific manner.

Methodological considerations of neurochemical imaging with ^{75}Se

The suitability of a radioisotope for *in vivo* tracer studies is determined by the physical properties of its radioactive decay. The half-life of 119.8 days and the properties of the emitted radiation of ^{75}Se are indeed very appropriate for such studies. First, the radioactive decay data of this radionuclide allows detection limits that cannot be reached with other analytical methods. Due to the high detection efficiency of radioanalytical methods, single atoms of radionuclides can be identified, whereas other element analytical methods often require a million or more atoms for detection (Adelstein & Manning 1995). In humans, the application of ^{75}Se was mostly related to cancer studies using this radiotracer as a tumor marker in general (Cavalieri *et al.* 1966; D'Angio *et al.* 1969). In studies using rodents the size of the typically investigated samples, i.e. whole organs, was limited by the geometry requirements of the detector allowing only the investigation of separated gross anatomical regions of the brain. In difference to such bulk analytical approaches our autoradiographic method enables a spatial resolution at the regional and cellular level which could be linked to histological features of the investigated tissue. In a comparable approach by Trapp and Millam (1975) the ^{75}Se distribution in the central nervous system was addressed but lack of spatial resolution restricted the measure to gross anatomical systems such as cortex without further regional refinement.

Selenium homeostasis in the brain is region-specific

In confirmation with earlier studies (Burk *et al.* 1972) we could show that the absorbed amount of ^{75}Se into the brain depends on the selenium status and shows a significant higher quantity in selenium deficient rats. Here, we could show that Se is region-specifically distributed in the brain. Se was enriched in certain grey matter regions, in particular hippocampus, cortex, and in granule cell layers of the cerebellum,

1
2
3 Neurochemical imaging of selenium in the brain
4
5

6 whereas other neuron-rich structures such as striatum or septum showed only low Se
7 levels. Thus, our data indicate that Se uptake and incorporation follows a certain
8 regional specificity indicating a distinct function of Se and selenoproteins in these brain
9 regions. Recently, we revealed that these regions indeed express also most of the 24
10 known murine selenoprotein mRNAs at high level (Zhang et al., 2007). Gene disruption
11 or RNAi mediated silencing of some selenoproteins such as glutathione peroxidase 1
12 (de Haan et al., 1998), glutathione peroxidase 4 (Yant et al., 2003; Borchert et al.,
13 2006), thioredoxine reductase 1 (Jakupoglu et al., 2005), or selenoprotein P (Hill et al.,
14 2003; Schomburg et al., 2003) have been shown to be essential for embryonic
15 development and proper neuronal function. In addition, in vitro studies indicated that
16 SEPW (Loflin et al., 2006), SEPR (Kryokov et al., 2002), GPx4 (Savaskan et al., 2007)
17 and SEP15 (Labunskyy et al., 2007) are implicated in cellular redox processes essential
18 for cell survival. Interestingly, we could show that all of these selenoproteins are
19 expressed in human, rat and mouse brain tissue, indicating that Se is required for
20 distinct brain regions.
21
22

23
24
25
26
27
28
29
30
31
32 However, remarkable high Se was found in choroid plexus irrespectively of the
33 nutritional Se status. Dietary selenium compounds (organic as well as inorganic
34 selenium forms) are taken up by intestinal resorption and are metabolized in the liver.
35 There, selenoprotein synthesis for such as plasma GPx and SePP takes place and are
36 secreted into the blood stream. In particular, among storage and organ-specific
37 functions, liver SEPP has been shown to transport Se in plasma, since SEPP is the only
38 selenoprotein known to date that contains multiple Sec residues (Motsenbocker &
39 Tappel, 1982; Hill et al., 1991; Renko et al., 2007). Recently, Burk et al. (2007) could
40 show that ApoER2^{-/-} mice have reduced Se levels in testis and brain and displayed
41 neurological defects similar to those found in SEPP^{-/-} mice, suggesting that ApoER2
42 functions as a SEPP receptor for these organs. However, mice with disrupted
43 selenoprotein expression (including SEPP) in liver through targeted tRNA^{[Sr]Sec} deletion
44 (the gene coding for the selenocysteine tRNA) still remained normal Se levels and
45 SEPP expression in the brain (Schweizer et al., 2005), implicating that SEPP has also
46 local Se scavenger and storage function. Interestingly, selenoprotein P has been shown
47 to be expressed in ependymal cells, the main cellular constituents of the choroid plexus
48
49
50
51
52
53
54
55
56
57
58
59
60

1
2
3 Neurochemical imaging of selenium in the brain
4
5

6 (Scharpf et al., 2007). Within the choroid plexus, the CSF is produced by ependymal
7 cells and released into the local environment, thereby providing the brain and spinal
8 cord with SEPP and subsequently with the trace element itself. Indeed, the choroid
9 plexus plays a prominent role in regulating of the homeostasis of other trace elements
10 such as zinc (Wang *et al.* 2004) and manganese (Takeda *et al.* 1994). Since our data
11 demonstrate that high levels of Se are retained in choroid plexus in selenium deficient
12 as well as selenium adequate rats, this structure might be essential for Se homeostasis
13 for the whole central nervous system.
14
15
16
17
18
19

20 In summary, we could show that Se is distributed in the brain in a region-specific
21 manner. We identified in particular the hippocampus, cortex, olfactory bulb, and
22 cerebellum as Se privileged regions which points most probably to the requirement of
23 certain selenoproteins for proper brain function. Under low Se status, increased
24 selenium uptake occurred in all regions of the grey matter. The choroid plexus retained
25 remarkably high Se incorporation irrespectively of the nutritional status, indicating a key
26 structure for Se homeostasis. Taken together, we investigated the distribution of the
27 trace element Se and selenoproteins in the brain under different nutritional conditions
28 and thus provide important data on Se and selenoprotein metabolism and its relation to
29 distinct brain regions.
30
31
32
33
34
35
36
37
38
39
40
41
42
43
44
45
46
47
48
49
50
51
52
53
54
55
56
57
58
59
60

1
2
3 *Neurochemical imaging of selenium in the brain*
4
5

6 **Acknowledgements**
7

8 We thank D. Behne and M. Kühbacher (HMI, Berlin) for providing materials and
9 technical support. This study was supported by the Deutsche Forschungsgemeinschaft
10 (DFG SPP1087, SA-1041/3-2 to N.E.S.), The International Human Frontier Science
11 Program Organisation (HFSP, to N.E.S.), the Köln Fortune Program (E.H.), and the
12 Wilhelm Sander-Stiftung (I.Y.E.).
13
14
15
16
17
18
19
20
21
22
23
24
25
26
27
28
29
30
31
32
33
34
35
36
37
38
39
40
41
42
43
44
45
46
47
48
49
50
51
52
53
54
55
56
57
58
59
60

For Peer Review

1
2
3 Neurochemical imaging of selenium in the brain
4
5

6 **References**
7

8 Andersen, O. and Nielsen, J. B. (1994) Effects of simultaneous low-level dietary
9 supplementation with inorganic and organic selenium on whole-body, blood, and organ levels of
10 toxic metals in mice. *Environ Health Perspect*, **102 Suppl 3**, 321-324.
11

12 Andersen, O. M., Yeung, C. H., Vorum, H. et al. (2003) Essential role of the apolipoprotein E
13 receptor-2 in sperm development. *J Biol Chem*, **278**, 23989-23995.
14

15 Arthur JR, Nicol F, Mitchell JH, Beckett GJ. Selenium and iodine deficiencies and selenoprotein
16 function. *Biomed Environ Sci*. 1997 Sep;10(2-3):129-35.
17

18 Behne, D., Hilmert, H., Scheid, S., Gessner, H. and Elger, W. (1988) Evidence for specific
19 selenium target tissues and new biologically important selenoproteins. *Biochim Biophys Acta*,
20 **966**, 12-21.
21

22 Behne, D., Hofer, T., von Berswordt-Wallrabe, R. and Elger, W. (1982) Selenium in the testis of
23 the rat: studies on its regulation and its importance for the organism. *J Nutr*, **112**, 1682-1687.
24

25 Behne, D., Weiss-Nowak, C., Kalcklosch, M., Westphal, C., Gessner, H. and Kyriakopoulos, A.
26 (1994) Application of nuclear analytical methods in the investigation and identification of new
27 selenoproteins. *Biol Trace Elem Res*, **43-45**, 287-297.
28

29 Berry, M. J., Banu, L., Chen, Y. Y., Mandel, S. J., Kieffer, J. D., Harney, J. W. and Larsen, P. R.
30 (1991) Recognition of UGA as a selenocysteine codon in type I deiodinase requires sequences
31 in the 3' untranslated region. *Nature*, **353**, 273-276.
32

33 Borchert A, Wang CC, Ufer C, Schiebel H, Savaskan NE, Kuhn H. The role of phospholipid
34 hydroperoxide glutathione peroxidase isoforms in murine embryogenesis. *J Biol Chem*. 2006 Jul
35 14;281(28):19655-64
36

37 Burk, R. F., Brown, D. G., Seely, R. J. and Scaief, C. C., 3rd (1972) Influence of dietary and
38 injected selenium on whole-body retention, route of excretion, and tissue retention of ⁷⁵SeO₃²⁻
39 in the rat. *J Nutr*, **102**, 1049-1055.
40

41 Burk, R. F. and Hill, K. E. (1994) Selenoprotein P. A selenium-rich extracellular glycoprotein. *J*
42 *Nutr*, **124**, 1891-1897.
43

44 Burk, R. F. and Hill, K. E. (2005) Selenoprotein P: an extracellular protein with unique physical
45 characteristics and a role in selenium homeostasis. *Annu Rev Nutr*, **25**, 215-235.
46

47 Burk, R. F., Hill, K. E., Olson, G. E., Weeber, E. J., Motley, A. K., Winfrey, V. P. and Austin, L.
48 M. (2007) Deletion of apolipoprotein E receptor-2 in mice lowers brain selenium and causes
49 severe neurological dysfunction and death when a low-selenium diet is fed. *J Neurosci*, **27**,
50 6207-6211.
51

52 Caban, K. and Copeland, P. R. (2006) Size matters: a view of selenocysteine incorporation from
53 the ribosome. *Cell Mol Life Sci*, **63**, 73-81.
54

Neurochemical imaging of selenium in the brain

Castellano, S., Morozova, N., Morey, M., Berry, M. J., Serras, F., Corominas, M. and Guigo, R. (2001) In silico identification of novel selenoproteins in the *Drosophila melanogaster* genome. *EMBO Rep*, **2**, 697-702.

Cavalieri, R. R., Scott, K. G. and Sairenji, E. (1966) Selenite (^{75}Se) as a tumor-localizing agent in man. *J Nucl Med*, **7**, 197-208.

Chen, J. and Berry, M. J. (2003) Selenium and selenoproteins in the brain and brain diseases. *J Neurochem*, **86**, 1-12.

D'Angio, G. J., Loken, M. and Nesbit, M. (1969) Radionuclear (^{75}Se) identification of tumor in children with neuroblastoma. *Radiology*, **93**, 615-617.

de Haan, J. B., Bladier, C., Griffiths, P. et al. (1998) Mice with a homozygous null mutation for the most abundant glutathione peroxidase, Gpx1, show increased susceptibility to the oxidative stress-inducing agents paraquat and hydrogen peroxide. *J Biol Chem*, **273**, 22528-22536.

Eyüpoglu IY, Hahnen E, Buslei R, Siebzehnrübl FA, Savaskan NE, Lüders M, Tränkle C, Wick W, Weller M, Fahlbusch R, Blümcke I. Suberoylanilide hydroxamic acid (SAHA) has potent anti-glioma properties in vitro, ex vivo and in vivo. *J Neurochem*. 2005; **93**(4):992-9.

Hatfield DL, Gladyshev VN. How selenium has altered our understanding of the genetic code. *Mol Cell Biol*. 2002 Jun; **22**(11):3565-76.

Hill KE, Lloyd RS, Yang JG, Read R, Burk RF. The cDNA for rat selenoprotein P contains 10 TGA codons in the open reading frame. *J Biol Chem*. 1991; **266**(16):10050-3.

Hill, K. E., Zhou, J., McMahan, W. J., Motley, A. K., Atkins, J. F., Gesteland, R. F. and Burk, R. F. (2003) Deletion of selenoprotein P alters distribution of selenium in the mouse. *J Biol Chem*, **278**, 13640-13646.

Hill, K. E., Zhou, J., McMahan, W. J., Motley, A. K. and Burk, R. F. (2004) Neurological dysfunction occurs in mice with targeted deletion of the selenoprotein P gene. *J Nutr*, **134**, 157-161.

Jakupoglu C, Przemecck GK, Schneider M, Moreno SG, Mayr N, Hatzopoulos AK, de Angelis MH, Wurst W, Bornkamm GW, Brielmeier M, Conrad M. Cytoplasmic thioredoxin reductase is essential for embryogenesis but dispensable for cardiac development. *Mol Cell Biol*. 2005; **25**(5):1980-8

Klivenyi, P., Andreassen, O. A., Ferrante, R. J. et al. (2000) Mice deficient in cellular glutathione peroxidase show increased vulnerability to malonate, 3-nitropropionic acid, and 1-methyl-4-phenyl-1,2,5,6-tetrahydropyridine. *J Neurosci*, **20**, 1-7.

Kryukov GV, Kumar RA, Koc A, Sun Z, Gladyshev VN. Selenoprotein R is a zinc-containing stereo-specific methionine sulfoxide reductase. *Proc Natl Acad Sci U S A*. 2002; **99**(7):4245-50

Kryukov, G. V., Castellano, S., Novoselov, S. V., Lobanov, A. V., Zehtab, O., Guigo, R. and Gladyshev, V. N. (2003) Characterization of mammalian selenoproteomes. *Science*, **300**, 1439-1443.

Neurochemical imaging of selenium in the brain

Labunskyy VM, Hatfield DL, Gladyshev VN. The Sep15 protein family: roles in disulfide bond formation and quality control in the endoplasmic reticulum. *IUBMB Life*. 2007 Jan;59(1):1-5.

Lescure, A., Gautheret, D., Carbon, P. and Krol, A. (1999) Novel selenoproteins identified in silico and in vivo by using a conserved RNA structural motif. *J Biol Chem*, **274**, 38147-38154.

Loflin, J., Lopez, N., Whanger, P. D. and Kioussi, C. (2006) Selenoprotein W during development and oxidative stress. *J Inorg Biochem*, **100**, 1679-1684.

Motsenbocker, M. A. and Tappel, A. L. (1984) Effect of dietary selenium on plasma selenoprotein P, selenoprotein P1 and glutathione peroxidase in the rat. *J Nutr*, **114**, 279-285.

Ramaekers, V. T., Calomme, M., Vanden Berghe, D. and Makropoulos, W. (1994) Selenium deficiency triggering intractable seizures. *Neuropediatrics*, **25**, 217-223.

Renko K, Werner M, Renner-Müller I, Cooper TG, Yeung CH, Hollenbach B, Scharpf M, Köhrle J, Schomburg L, Schweizer U. Hepatic selenoprotein P (SePP) expression restores selenium transport and prevents infertility and motor-incoordination in Sepp-knockout mice. *Biochem J*. 2008 Feb 1;409(3):741-9

Saijoh, K., Saito, N., Lee, M. J., Fujii, M., Kobayashi, T. and Sumino, K. (1995) Molecular cloning of cDNA encoding a bovine selenoprotein P-like protein containing 12 selenocysteines and a (His-Pro) rich domain insertion, and its regional expression. *Brain Res Mol Brain Res*, **30**, 301-311.

Savaskan, N. E., Borchert, A., Brauer, A. U. and Kuhn, H. (2007) Role for glutathione peroxidase-4 in brain development and neuronal apoptosis: Specific induction of enzyme expression in reactive astrocytes following brain injury. *Free Radic Biol Med*, **43**, 191-201.

Savaskan, N. E., Brauer, A. U., Kuhbacher, M., Eyupoglu, I. Y., Kyriakopoulos, A., Ninnemann, O., Behne, D. and Nitsch, R. (2003) Selenium deficiency increases susceptibility to glutamate-induced excitotoxicity. *FASEB J*, **17**, 112-114.

Scharpf, M., Schweizer, U., Arzberger, T., Roggendorf, W., Schomburg, L. and Köhrle, J. (2007) Neuronal and ependymal expression of selenoprotein P in the human brain. *J Neural Transm*, **114**, 877-884.

Schomburg, L., Schweizer, U., Holtmann, B., Flohe, L., Sendtner, M. and Köhrle, J. (2003) Gene disruption discloses role of selenoprotein P in selenium delivery to target tissues. *Biochem J*, **370**, 397-402.

Schweizer, U., Brauer, A. U., Köhrle, J., Nitsch, R. and Savaskan, N. E. (2004a) Selenium and brain function: a poorly recognized liaison. *Brain Res Brain Res Rev*, **45**, 164-178.

Schweizer, U., Schomburg, L. and Savaskan, N. E. (2004b) The neurobiology of selenium: lessons from transgenic mice. *J Nutr*, **134**, 707-710.

Schweizer, U., Streckfuss, F., Pelt, P., Carlson, B. A., Hatfield, D. L., Köhrle, J. and Schomburg, L. (2005) Hepatically derived selenoprotein P is a key factor for kidney but not for brain selenium supply. *Biochem J*, **386**, 221-226.

1
2
3 Neurochemical imaging of selenium in the brain
4
5
6

7 Spector, R. (1989) Micronutrient homeostasis in mammalian brain and cerebrospinal fluid. *J*
8 *Neurochem*, **53**, 1667-1674.
9

10 Takeda, A., Akiyama, T., Sawashita, J. and Okada, S. (1994) Brain uptake of trace metals, zinc
11 and manganese, in rats. *Brain Res*, **640**, 341-344.
12

13 Trapp, G. A. and Millam, J. (1975) The distribution of ⁷⁵Se in brains of selenium-deficient rats. *J*
14 *Neurochem*, **24**, 593-595.
15

16 Wang, Z. Y., Stoltenberg, M., Jo, S. M., Huang, L., Larsen, A., Dahlstrom, A. and Danscher, G.
17 (2004) Dynamic zinc pools in mouse choroid plexus. *Neuroreport*, **15**, 1801-1804.
18

19 Yant LJ, Ran Q, Rao L, Van Remmen H, Shibatani T, Belter JG, Motta L, Richardson A, Prolla
20 TA. The selenoprotein GPX4 is essential for mouse development and protects from radiation
21 and oxidative damage insults. *Free Radic Biol Med*. 2003;34(4):496-502
22

23 Zhang Y, Zhou Y, Schweizer U, Savaskan NE, Hua D, Kipnis J, Hatfield DL, Gladyshev VN.
24 Comparative analysis of selenocysteine machinery and selenoproteome gene expression in
25 mouse brain identifies neurons as key functional sites of selenium in mammals. *J Biol Chem*.
26 2008;283(4):2427-38.
27
28
29
30
31
32
33
34
35
36
37
38
39
40
41
42
43
44
45
46
47
48
49
50
51
52
53
54
55
56
57
58
59
60

1
2
3 Neurochemical imaging of selenium in the brain
4
5

6 **Figure legends**
7

8
9 **Figure 1: Effects of low selenium diet on ^{75}Se distribution in the brain. **A, B,**
10 Autoradiogram of representative brain sections from rats with the selenium-adequate diet
11 (Se+) and selenium deficient diet (Se-). Both groups were radiolabeled with ^{75}Se for
12 seven days. Arrows indicate choroid plexus. Scale bar represents 5 mm. Numbers mark
13 the following regions: 1, dentate gyrus; 2, entorhinal cortex; 3, CA1; 4, CA3; 5, choroid
14 plexus; 6, cortex; 7, anterior commissure; 8, septum; 9, molecular layer; 10, granule cell
15 layer.
16
17
18
19
20
21**

22
23 **Figure 2: Neurochemical imaging and analysis of selenium distribution in the**
24 **brain.** Quantitative autoradiographic evaluation of brain sections from selenium-
25 adequate (Se+) and selenium deficient rats (Se-). **A,** Photomicrograph of a horizontal
26 brain section from a selenium deficient rat, labeled for seven days with ^{75}Se . The Nissl
27 staining was applied after the autoradiographic procedure. Numbers indicate areas of
28 quantitative evaluation. **B,** Autoradiogram of the same sample. The color code bar
29 illustrates the coding scheme for the ^{75}Se activity. Scale bar represents 5 mm. **C,**
30 Quantitative analysis of the ^{75}Se activity per area in 10 distinct brain regions of selenium
31 deficient and adequate rats. Note, that especially neuron rich areas (grey matter) such
32 as CA1-3, septum and cortex are enriched in selenium accumulation. Choroid plexus
33 and granule cell layer in the cerebellum give highest signals. The values are expressed
34 as percentage of relative ^{75}Se activity/area (mean \pm SD). Scale bar represents 5mm.
35
36
37
38
39
40
41
42
43
44

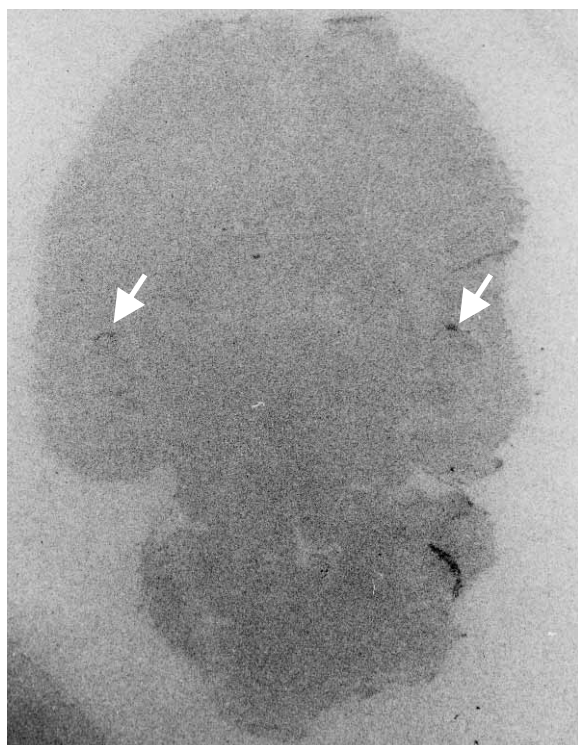
45 **Figure 3: Neurochemical imaging of the selenium privileged organ testis. **A,****
46 **Autoradiogram of a 12 μm thick section of testis and the epididymidis obtained from**
47 **selenium deficient rats after 7 days of ^{75}Se radiotracer application. The color code bar**
48 **represents the quantitative coding scheme for ^{75}Se activity. Scale bar is 5 mm. **B,****
49 **Quantitative analysis of the ^{75}Se activity per area in distinct areas of testis in selenium**
50 **deficient rats. Note, that especially seminiferous tubules show enriched selenium**
51 **accumulation. The values are expressed as percentage of relative ^{75}Se activity/area.**
52
53
54
55
56
57
58
59
60

1
2
3 Neurochemical imaging of selenium in the brain
4
5

6 **Figure 4: Microarray analysis of the rat hippocampal selenoprotein gene**
7 **expression.** Selenoprotein gene expression in the rat hippocampus was determined by
8 Affymetrix RAE230 microarray analysis performed in triplicate. 19 selenoprotein genes
9 with significant expression levels could be identified. Red line defines the mean
10 selenoprotein gene expression level. The low variability of housekeeping gene
11 expression (GAPDH, hexokinase) indicates the reproducibility of the assays performed.
12
13
14
15
16
17

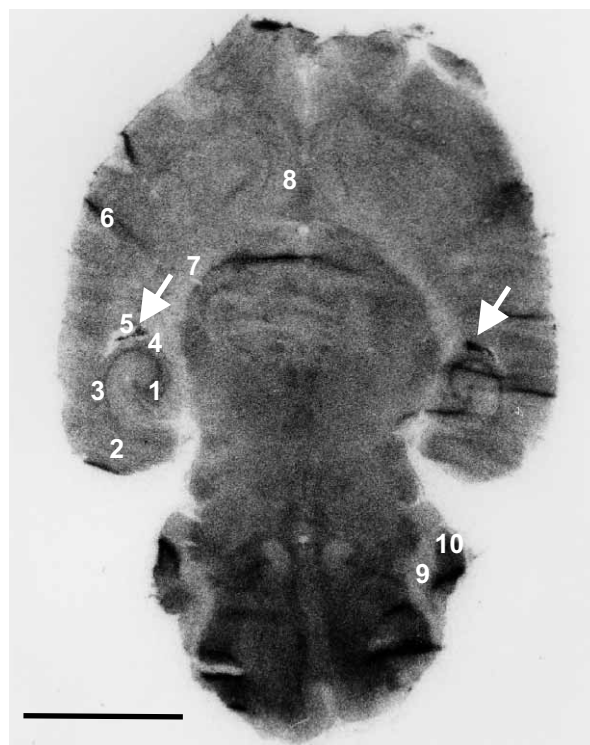
18 **Figure 5: Analysis of the selenoprotein gene expression in humans and rodent**
19 **hippocampi. A,** Selenoprotein gene expression in hippocampus determined by RT-
20 PCR analysis. Expression of eight selenoprotein genes was confirmed in the human, rat
21 and mouse hippocampus. **B,** GPx4 profile in the brain. GPx4 is neuron-specifically
22 expressed in the brain. Confocal image of GPx4 immunostained rat brain section.
23 Arrows mark immunopositive pyramidal neurons, arrow heads indicate dendrites. Scale
24 bar represents 10 μm .
25
26
27
28
29
30
31
32
33
34
35
36
37
38
39
40
41
42
43
44
45
46
47
48
49
50
51
52
53
54
55
56
57
58
59
60

A



Se (+)

B



Se (-)

Peer Review

1
2
3
4
5
6
7
8
9
10
11
12
13
14
15
16
17
18
19
20
21
22
23
24
25
26
27
28
29
30
31
32
33
34
35
36
37
38
39
40
41
42
43
44
45
46
47
48
49
50
51
52
53
54
55
56
57
58
59
60

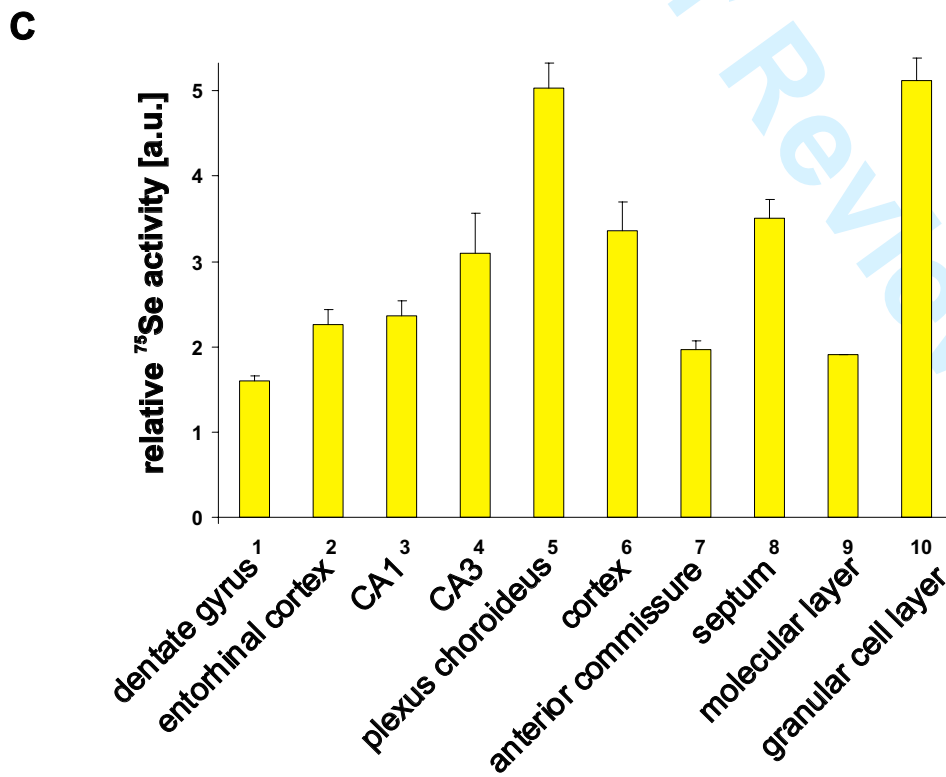
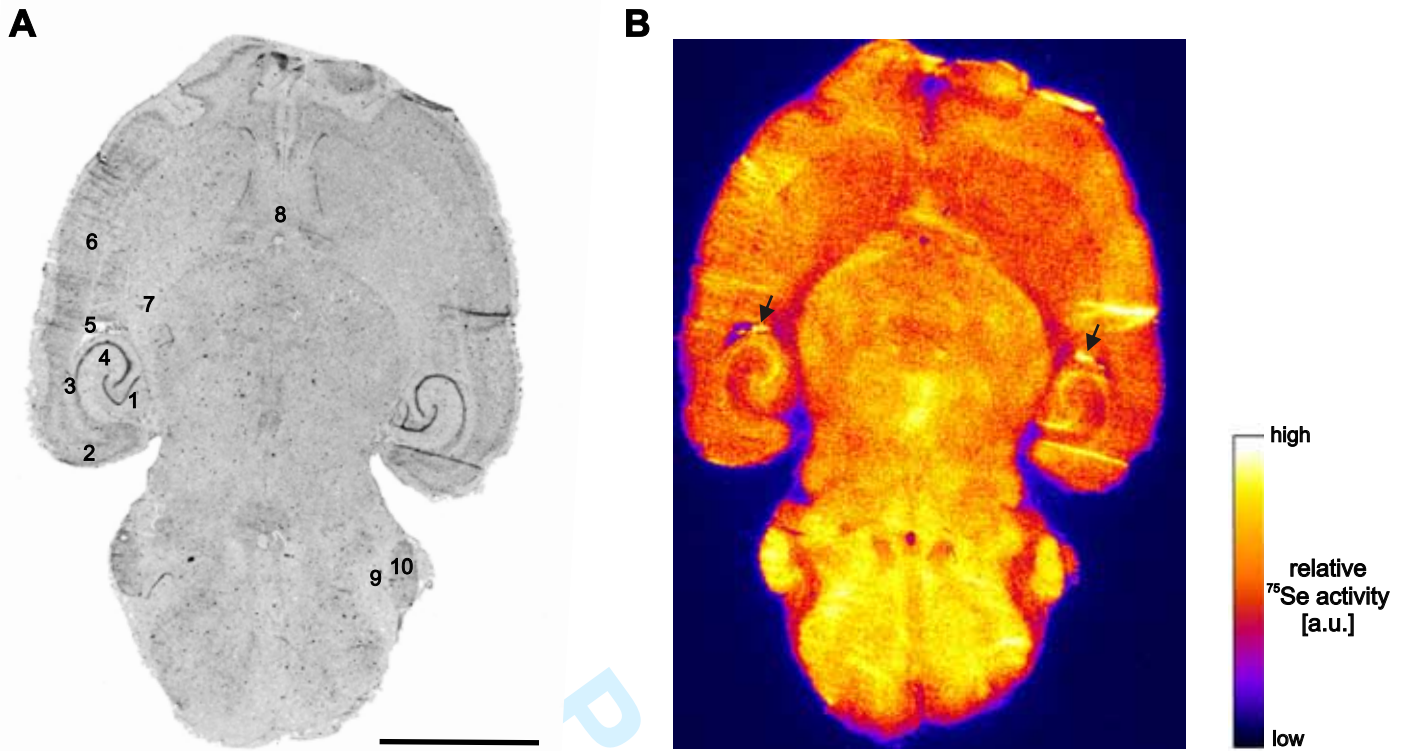
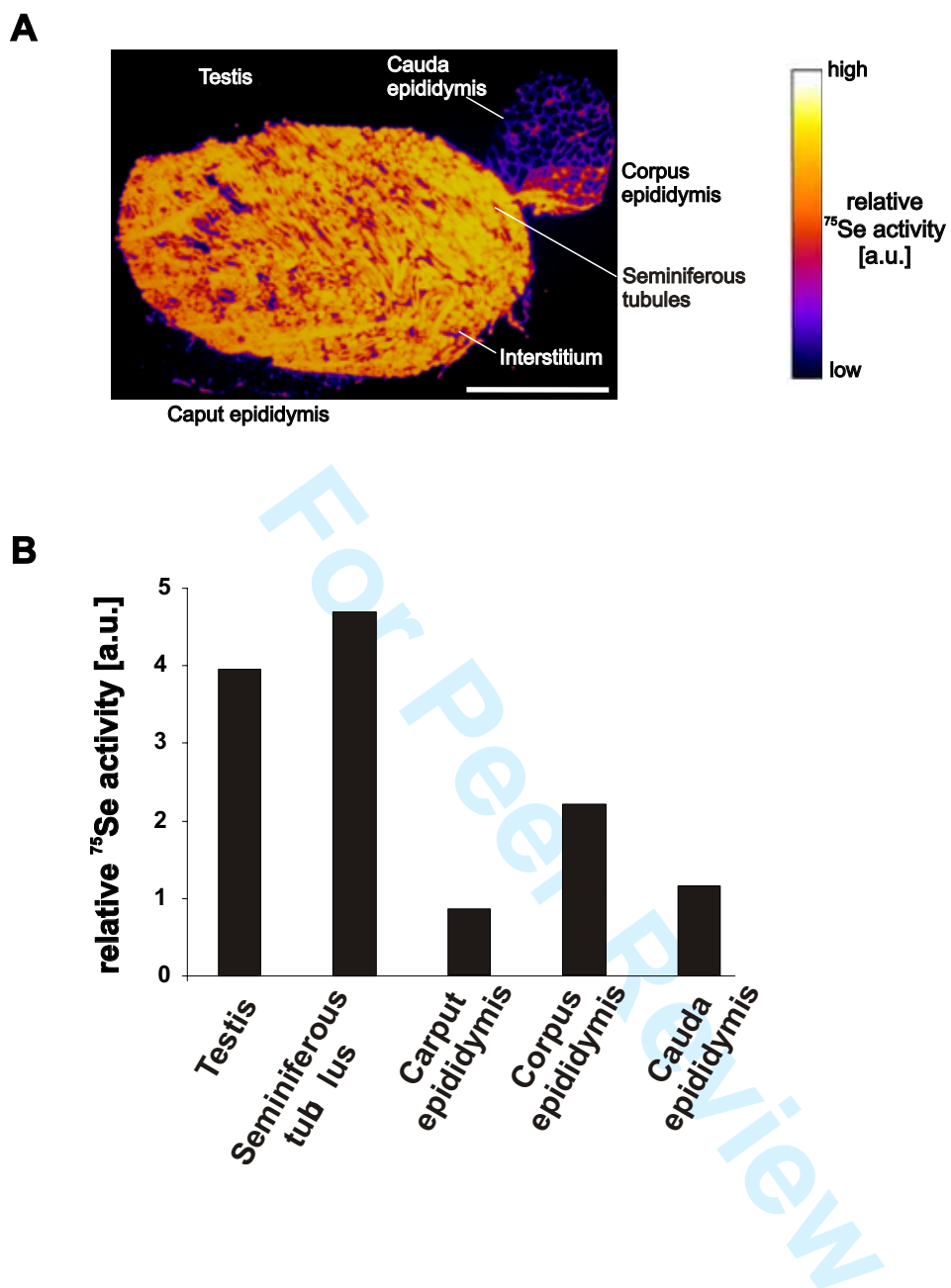
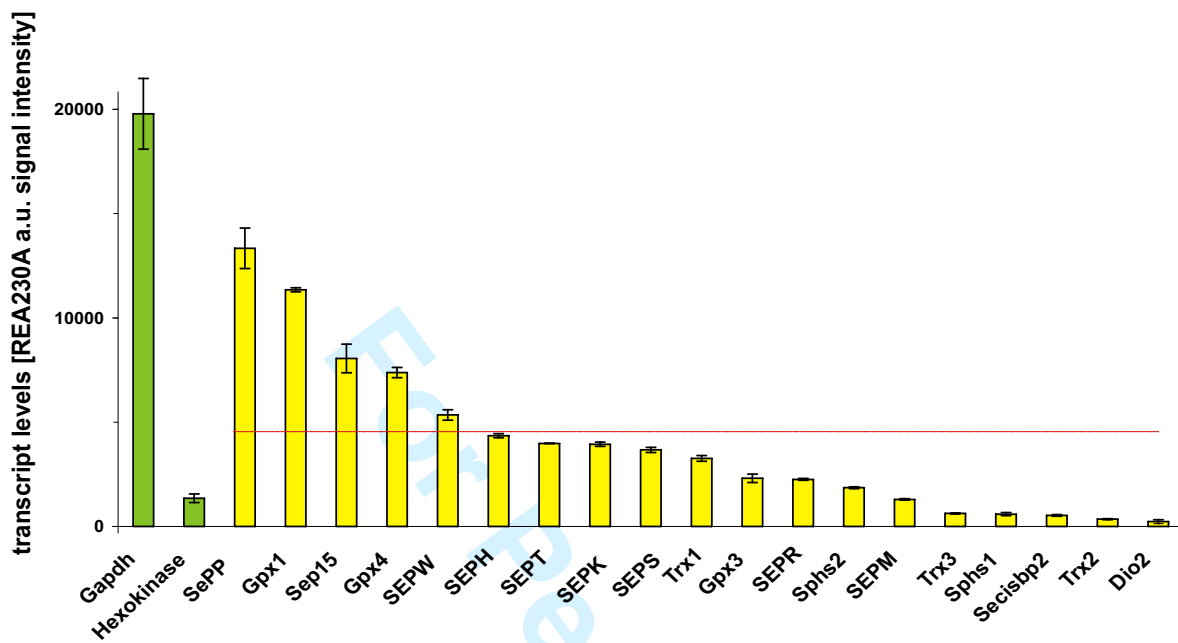


Figure 3

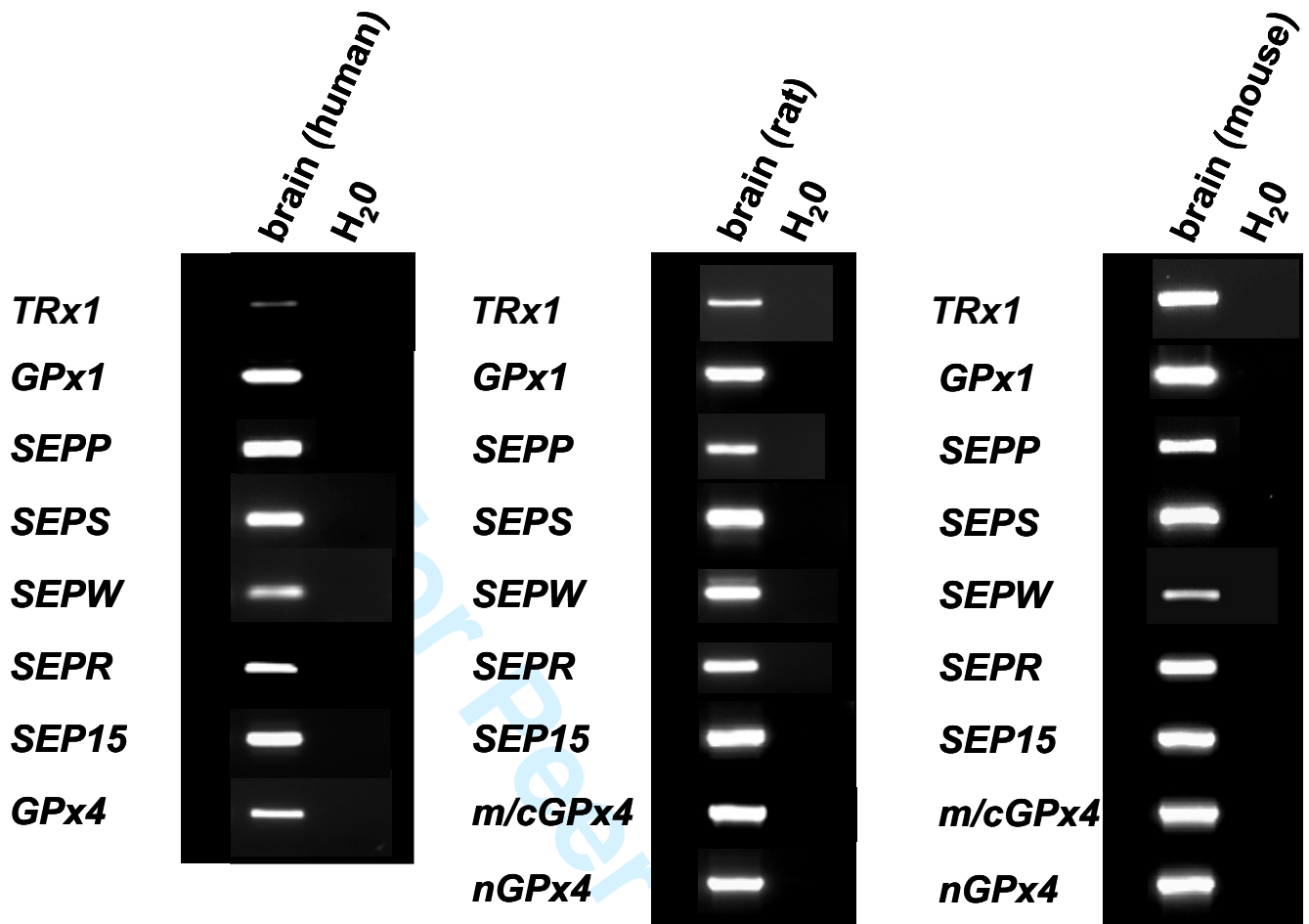




1
2
3
4
5
6
7
8
9
10
11
12
13
14
15
16
17
18
19
20
21
22
23
24
25
26
27
28
29
30
31
32
33
34
35
36
37
38
39
40
41
42
43
44
45
46
47
48
49
50
51
52
53
54
55
56
57
58
59
60

Figure 5

A



B

